Radiation Measurements 90 (2016) 292–297

Contents lists available at ScienceDirect

Radiation Measurements

journal homepage: www.elsevier.com/locate/radmeas

Probing luminescence centers in Na rich feldspar

A.K. Prasad*, T. Lapp, M. Kook, M. Jain

Center for Nuclear Technologies, Technical University of Denmark, DTU Risø Campus, Roskilde 4000, Denmark

HIGHLIGHTS

- The UV, violet–blue, green and deep red emissions characterised using site-selective spectroscopy.
- The green–yellow band shifts with the excitation energy and is not related to Mn^{2+}.
- Band-tail states likely play a role in the green and deep red PL emissions.

ARTICLE INFO

Article history:
Received 25 October 2015
Received in revised form
27 February 2016
Accepted 29 February 2016
Available online 2 March 2016

Keywords:
Na-feldspar
X-ray excited optical luminescence
Radioluminescence
Photoluminescence
Band-tail model

ABSTRACT

In contrast to the detailed investigations on the dosimetric electron trap in feldspar only little has been done to understand the luminescence centers. We use a comparison of multiple spectroscopic techniques, site selective photoluminescence spectroscopy and time resolved measurements to further our understanding of the luminescence mechanisms and recombination sites, in a sample of Na rich plagioclase feldspar (oligoclase). Both the UV and violet–blue emissions show resonant excitations arising from a distribution of energy levels. We propose, contrary to the general understanding, that the green emission may not arise from Mn^{2+} in our sample and that photoionisation of this centre may be possible by excitation to the band tail states. The deep red emission is tied to the Fe^{3+}, and the exponential rise in the UV excitation efficiency of this centre is discussed in the context of the band-tail model.

1. Introduction

The photoemissions from feldspars are widely used in retrospective dosimetry and optical dating of geological and archaeological events (Huntley et al., 1985; Jain, 2014; Krbetschek et al., 1997; Sohbati et al., 2013). Feldspars are ubiquitous in nature, and the dosimetric signal measured as infra-red stimulated luminescence (IRSL) shows growth up to 1 kGy dose range, allowing reconstruction of geological history up to about 0.5 Ma. However, this signal suffers from anomalous, athermal fading. A large body of work exists on the dosimetric, electron trapping centre which gives rise to this IRSL signal (Hutt et al., 1988; Poolton & Bailiff, 1989; Jain & Ankjærgaard, 2011; Andersen et al., 2012; Kars et al., 2013; Jain et al., 2015 etc.); these studies include both the tunnelling behaviour and the mapping of the energy level within the band gap. In contrast, only little has been done to characterise the recombination centers. Based on spectral characteristics of feldspars (Krbetschek et al., 1997), it is inferred that the UV emission arises from an intrinsic defect (Garcia-Guinea et al., 1999), the blue emission, common to most feldspars, from a hole-bearing oxygen atom adjacent to two Al atoms ($Al–O^{-}–Al$) (Finch & Klein, 1999), the green–orange emission, characteristic of some Na-feldspars, from Mn^{2+} luminescence centre occupying Ca sites (Geake et al., 1977), and the deep red emission band from tetrahedral Fe^{3+} ($^4T_1 \rightarrow {}^6A_1$ transition) substituting for Al^{3+} (Geake et al., 1977; Telfer & Walker, 1975; White et al., 1986). A more comprehensive characterisation of the recombination centers is lacking. For example, there is little understanding of the distribution as well as the positions of the energy levels of these defects within the band gap. Similarly, there is little information on the characteristic fluorescence/phosphorescence lifetimes of these emissions.

The objective of this study is to further understand the luminescence transitions within the recombination centers in feldspars, and explore their energy structure and distribution within the bandgap. A special focus is given on the green and deep red emission. We use a combination of probing methods: X-rays in keV regime (X-ray excited optical luminescence: XEOL), Sr^{90}/Y^{90} beta particles (radioluminescence: RL) and UV–VIS–IR photons

* Corresponding author.
E-mail address: akpr@dtu.dk (A.K. Prasad).

http://dx.doi.org/10.1016/j.radmeas.2016.02.033
1350-4487/

(photoluminescence: PL). These beta and X-ray excitations directly ionize the host lattice because the incident energy is much higher than the band gap of the feldspars ~7.7 eV (Poolton et al., 2006) leading to electron–hole recombination at the luminescence centers. In contrast, the optical excitation (PL; 1.9 eV – 4.86 eV) allows the possibility of probing the energy structure of these centers and possibly their disposition within the band gap using site selective spectroscopy. We also report on the luminescence lifetimes on microsecond and millisecond time scales characteristic of these centres.

2. Instrumentation and sample

We measured a set of feldspar museum specimens reported previously by Ankjærgaard et al. (2009) and Morthekai et al. (2013) using RL and PL. Of these a representative oligoclase sample (Oligoclase 1 of Morthekai et al., 2013) was chosen for detailed studies presented here as this sample had relatively higher optical sensitivity compared to the other samples, and showed all the typical bands reported for feldspars (Krbetschek et al., 1997). The main cationic constituents of the sample are (in molar %): Na-73.7, Ca-18.9 and K-7.4; their concentrations were measured using inductively coupled plasma mass spectrometry (ICP-MS; Morthekai et al., 2013). The grain size used in the present studies was in the range of 90–180 μm.

To measure the RL, the sample was mounted with a silicon oil into the steel cup and placed in the Risø TL/OSL Reader (Model DA 20) equipped with a Sr^{90}/Y^{90} beta source (dose rate 0.1 Gy/s). The signal was collected through a fibre bundle; the circular (3 mm ϕ) end of the bundle looked at the sample under the beta source, while the other end arranged in an array of two rows was coupled to the Shamrock 193i spectrograph which dispersed the spectra on a high sensitivity EMCCD (iXon Ultra 888). The RL spectra were recorded from 250 nm to 1050 nm by setting the 300 lines/mm grating in four overlapping positions. The RL spectra were corrected for the spectral functions of grating, optical fibre and EMCCD.

The photoluminescence spectra were measured using Horiba Fluorolog-3 spectrofluorometer. A 450 W Xenon CW lamp was used for excitation within a wavelength range of approximately 255 nm–600 nm, with required wavelengths selected using a double grating Cherny-Turner excitation monochromator. Emission spectra in the range of 290 nm–600 nm were measured with a double grating Cherny-Turner spectrometer equipped with a photomultiplier tube (PMT). Spectra from 620 nm to 1000 nm were measured with Jobin-Yvon, HR-320 spectrometer (300 lines/mm grating) coupled to a liquid nitrogen cooled CCD detector, because of better efficiency of the CCD compared to PMT in the red-IR region. All spectra were corrected for the instrument response and photon flux. Appropriate long-pass filters were placed between the sample and the emission monochromator to remove second order diffraction of the primary excitation light. The PL phosphorescence decay was measured with the pulsed Xe-lamp placed in the same housing as the CW-lamp. The required wavelength of the excitation pulses was selected with the excitation monochromator and emission was recorded with the emission monochromator. The integration time of the emission collection was 100 ms and the initial delay of the system was 0.05 ms; all the measurements used flash counts of 100 to improve counting statistics.

XEOL was measured using a 40 kV X-ray tube installed on Horiba Fluorolog-3 spectrofluorometer. The X-ray tube was operated at 39.7 kV anode voltage and 95.7 mA anode current, and sample chamber pressure of 2.3×10^{-4} mB (vacuum was used because of interlock constraints). All low temperature luminescence measurements were accomplished in the same system using variable temperature (7–300 K) closed loop He cryostat operated with a sample chamber pressure at 2.4×10^{-5} mB, integrated into the Horiba emission/excitation spectrofluorometer. The proportional integral-derivative (PID) temperature control is provided through a Lakeshore (model 335) control unit. The sample grains were directly mounted on a copper-based sample holder (a cold finger) with the help of carbon tape.

3. Comparison of the XEOL, PL and RL spectra

Fig. 1 shows comparison of normalised XEOL, PL and RL spectra of our oligoclase sample. Four broad emission peaks can be observed at around 1.70, 2.2, 3.1 and 3.8 eV. The XEOL and the RL data are broadly similar, suggesting the same mechanism for both these cases; this is not surprising since both the 40 kV X-rays and the high-energy beta particles (mean energy 600 keV) have energy higher than the band gap and access the entire sample volume. However, there is a hump at about 2.5 eV in the RL spectra which is not present in XEOL; it needs to be confirmed if this hump is real or it is a measurement artefact.

In contrast to the RL/PL spectra, the relative intensity of the 2.2 eV peak is strongly subdued in the PL spectra, suggesting that the optical cross-section of the green emission centre is small compared to the other centers; this, however, is not an issue in RL and XEOL as the electron relaxation occurs from the conduction band in the latter mechanisms. The spectral bands observed in our work are in good agreement with the previous studies (Krbetschek et al., 1997).

4. Site selective photoluminescence spectra and luminescence lifetimes

PL excitation and emission spectra were measured to get further information about the energy structure of the defects giving rise to the above mentioned emission bands. The results are presented in Fig. 2a … (d) and discussed below:

4.1. UV emission

The black curve in Fig. 2a shows excitation spectrum for the emission at 3.86 eV. There is a broad, well defined excitation peak at 4.27 eV with a FWHM of ~0.4 eV. The blue curve shows the corresponding emission spectrum excited at 4.27 eV consisting of two

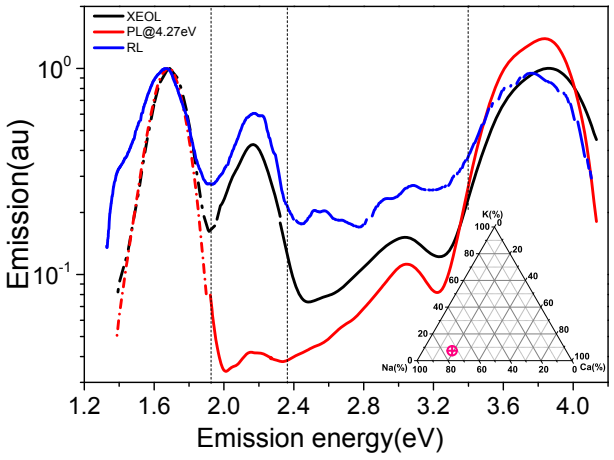

Fig. 1. A comparison of the XEOL (black), PL (Red) and RL (blue) spectra. In the case of XEOL and PL, the solid curves are the data collected through the PMT channel, whereas the dotted curves are collected using the CCD channel. A 610 nm long pass filter was used to avoid excitation scattered light for the collection of CCD data (For interpretation of the references to colour in this figure legend, the reader is referred to the web version of this article).